J. Plasma Physics (2005), *vol.* 71, *part* 2, *pp.* 217–224. © 2005 Cambridge University Press
DOI: 10.1017/S002237780400354X Printed in the United Kingdom

Electron energy distribution function in low-pressure complex plasmas

K. OSTRIKOV[1,3], I. DENYSENKO[2]†, M. Y. YU[2] and S. XU[3]

[1]School of Physics, The University of Sydney, Sydney, NSW 2006, Australia
(K.Ostrikov@physics.usyd.edu.au)

[2]Theoretical Physics I, Ruhr University, D-44780 Bochum, Germany
(deny@tp1.rub.de)

[3]Plasma Sources and Applications Center, NIE, Nanyang Technological University,
1 Nanyang Walk, 637616 Singapore

(Received 21 September 2004 and in revised form 19 November 2004)

Abstract. The effect of density and size of dust grains on the electron energy distribution function (EEDF) in low-temperature complex plasmas is studied. It is found that the EEDF depends strongly on the dust density and size. The behavior of the electron temperature can differ significantly from that of a pristine plasma. For low-pressure argon glow discharge, the Druyvesteyn-like EEDF often found in pristine plasmas can become nearly Maxwellian if the dust density and/or sizes are large. One can thus control the plasma parameters by the dust grains.

1. Introduction

Complex plasmas containing fine charged grains have attracted much attention in recent years [1–5]. Grain nucleation and agglomeration are often utilized in plasma-enhanced chemical vapor deposition (PECVD) for achieving fast deposition rates and atomic-to-mesoscopic structural transitions [6]. Dust grains are useful in fabricating nanostructured novel objects [2] and functional surfaces. On the other hand, presence of unwanted dusts often has a deleterious effect on the microstructuring of semiconductor wafers [7, 8]. The control, or management, of the dust grains in plasma devices is therefore crucial for plasma-assisted materials processing.

The electron energy distribution function (EEDF) is closely associated with the rates of the major elementary processes, particle and power balance in the discharge, and it determines the global stability and operational properties of the plasma [5, 9–12]. Control of the EEDF is thus one of the major challenges in the application of chemically active plasmas in the microelectronic and other industries [12, 13]. Prediction of the evolution of the EEDF is crucial for fine-tuning the complex plasma and much progress has recently been made [5, 14, 15].

It is widely accepted that the electron energy in dusty plasmas can be enhanced to unusual levels [6]. Fluid simulations have revealed higher ionization rates in dusty plasmas and this can be attributed to the stronger electric fields. Nevertheless, the relation between the effective electron temperature $T_{\rm eff} = \frac{2}{3}\langle\mathscr{E}\rangle$, where $\langle\mathscr{E}\rangle$ is the

† Permanent address: School of Physics and Technology, Kharkiv National University, 61077 Kharkiv, Ukraine.

https://doi.org/10.1017/S002237780400354X Published online by Cambridge University Press

average electron energy, and the dust density and size still remains controversial. Indeed, both increases [3,16] and decreases [17] in $T_{\rm eff}$ as compared with the pristine case have been reported. Different results have been obtained experimentally and numerically from pre-set EEDFs and/or fixed or floating $E_{\rm p}/N$ [3–5,18], where $E_{\rm p}$ is the plasma sustaining electric field and N is the density of neutrals.

A few questions still remain to be answered. First, is the average electron energy of dusty plasmas necessarily higher than that of the pristine plasma? Second, under what dust-specific conditions does $T_{\rm eff}$ increase or decrease? Third, what is the effect of the grains on the EEDF, and are the grains solely responsible for the EEDF profile? Fourth, can dusts be used to thermalize the plasma electrons and what is the role of the electron–dust collisions?

In this paper we attempt to resolve some of these issues by studying the effect of the dusts on the EEDF in a radiofrequency (RF) argon discharge. The main processes relevant to the energy balance of the system are included. It is shown that the presence of charged grains can significantly modify the EEDF by redistributing the high- and low-energy electrons. The evolution of $T_{\rm eff}$ in the plasma with growing total negative grain charge is numerically computed and interpreted in terms of $E_{\rm p}/N$ variations. Although the EEDF in the pristine plasma is Druyvesteyn-like, a pronounced presence of dusts can lead to electron thermalization (Maxwellization). The dependence of the main plasma parameters on the dust density and size is also investigated.

2. The model

We consider a RF low-pressure, high-density ($n_{\rm i} \geq 10^{10}$ cm^{-3}, where $n_{\rm i}$ is the ion number density in the dust-containing bulk plasma), cylindrical argon plasma of radius R and length L containing charged dust grains. The discharge is maintained by an electric field $E(t) \sim \exp(i\omega t)$, where $\omega = 2\pi f$, $f = 13.56$ MHz. The plasma is composed of electrons, singly charged positive ions Ar^+ and negatively charged dust grains. The dust grains are all of the same radius $a_{\rm d}$ and are uniformly distributed along the plasma column with density $n_{\rm d}$. The dust grains are absent in a boundary layer of thickness l adjacent to the wall. The spatial profile of the dust density $n_{\rm d}$ is chosen to fit that typical in dust-growth experiments [19] and is often observed when the grains were first created in the silane–argon mixture and then trapped in the argon discharge.

The shielding potential at a distance r from a grain may be approximated by the Debye–Hückel potential [2,5]: $\phi(r) = \phi_{\rm s}(a_{\rm d}/r)\exp(-r - a_{\rm d}/\lambda_{\rm DL})$, where the Debye length is $\lambda_{\rm DL}^{-2} = 4\pi e(n_{\rm e}/T_{\rm eff} + n_{\rm i}/2\mathscr{E}_{\rm i})$, with $\phi_{\rm s}$ the potential at the dust surface, $\mathscr{E}_{\rm i}$ (approximately 0.06 eV here) the average ion energy and $T_{\rm eff}$ the effective electron temperature. For a given EEDF $F_0(u)$, where u is the electron kinetic energy in eV, the electron current collected by a dust particle in the orbit-motion limited (OML) approximation is given by

$$I_{\rm e} = -\pi a_{\rm d}^2 e n_{\rm e} \int_{-\phi_{\rm s}}^{\infty} \left(1 + \frac{\phi_{\rm s}}{u}\right) \sqrt{\frac{2eu}{m_{\rm e}}} F_0(u) \sqrt{u}\, du, \tag{2.1}$$

where $n_{\rm e}$ is the bulk electron density and $m_{\rm e}$ is the electron mass. The ion current on a dust grain is $I_{\rm i} = \pi a_{\rm d}^2 e n_{\rm i} \sqrt{2e\mathscr{E}_{\rm i}/m_{\rm i}}\,(1 - \phi_{\rm s}/\mathscr{E}_{\rm i})$, where the dust surface potential $\phi_{\rm s}$ is related to the dust charge $eZ_{\rm d}$ by $\phi_{\rm s} = eZ_{\rm d}/a_{\rm d}$. We also assume constant dust charge, or $I_{\rm e} + I_{\rm i} = 0$, and quasineutrality $n_{\rm e} + n_{\rm d}|Z_{\rm d}| = n_{\rm i}$.

https://doi.org/10.1017/S002237780400354X Published online by Cambridge University Press

The isotropic part of F_0 is described by the Boltzmann equation [20, 21]

$$-\frac{2e}{3m_e}\frac{d}{du}\left(\frac{u^{3/2}}{\nu_m(u)}E_{eff}^2(u)\frac{dF_0}{du}\right) = S_{ea}(F_0) + S_{ee}(F_0) + S_{ed}(F_0), \tag{2.2}$$

where $E_{eff} = E_p\nu_m(u)/[2(\nu_m^2(u)+\omega^2)]^{1/2}$, E_p is the spatially averaged intensity of the electric field sustaining the plasma, $\nu_m(u)$ is the collision frequency for electron–neutral momentum transfer including electron–neutral and electron–dust collisions, and $S_{ea}(F_0)$, $S_{ed}(F_0)$, $S_{ee}(F_0)$ describe electron–atom, electron–dust and electron–electron collisions, respectively [15]. Electron–dust collisions are decribed by [17]

$$S_{ed}(F_0) = \frac{d}{du}\left[\frac{2m_e}{m_d}u^{3/2}\nu_{ed}^e\left(F_0 + T_d\frac{dF_0}{du}\right)\right] - \nu_{ed}^c F_0 u^{1/2}, \tag{2.3}$$

where $\nu_{ed}^e(u)$ and $\nu_{ed}^c(u)$ are the momentum transfer and the electron absorption frequencies of electron–dust collisions, respectively, and m_d and T_d are the mass and temperature of the dusts. For definitiveness, we set $T_d = 0.026$ eV and $m_d = (4/3)\rho_d\pi a_d^3$, where ρ_d is the grain material density (here, we have assumed $\rho_d = 2.0$ g cm^{-3}) [2]. The electron momentum transfer frequency can be written as [5,17]

$$\nu_{ed}^e(u) = \pi n_d\sqrt{2eu/m_e}\,a_d^2(-\phi_s/u)^2 e^{2a_d/\lambda_{DL}}\ln\Lambda, \tag{2.4}$$

where $\Lambda \approx -\lambda_{DL}T_{eff}/a_d\phi_s$. The electron–dust collection frequency is

$$\nu_{ed}^c(u) = \pi n_d\sqrt{2eu/m_e}\,a_d^2(1+\phi_s/u) \quad \text{for } u \geq -\phi_s, \tag{2.5}$$

and $\nu_{ed}^c(u) = 0$ for $u < -\phi_s$. Conservation of the ions (here Ar^+) requires $K_{iz}n_e n_g V - K_{id}n_d n_i V - n_{is}u_{Bi}S = 0$, where $u_{Bi} \approx \sqrt{2e/m_i}\,(\int_0^\infty F_0(u)u^{-1/2}\,du)^{-1/2}$ is the ion speed at the boundary of the bulk plasma and the sheath [22], S is the surface area of the chamber wall, K_{id} is the rate coefficient for ion–dust collisions ($K_{id}n_i = I_i/e$), K_{iz} is the ionization rate coefficient, and n_{is} is n_i at the sheath–bulk plasma boundary.

Power balance in the discharge requires [18] $P_{in} = P_{ea} + P_w + P_{dust}$, where P_{in} is the total power absorbed by the discharge and is an input parameter, P_{ea} is the energy loss via electron–neutral collisions, and P_w and P_{dust} is the power loss in the form of kinetic energy loss due to electrons and ions hitting the wall and dust grains, respectively. The power lost to the dust grains is $P_{dust} = eq_{ed}n_d V_{dust}$, where V_{dust} is the volume of the dusty plasma [18]. Here

$$q_{ed} = \pi a_d^2 n_e\int_{-\phi_s}^{\infty}\left(1+\frac{\phi_s}{u}\right)\sqrt{\frac{2eu}{m_e}}F_0 u^{3/2}\,du \tag{2.6}$$

is the heat flux associated with the electron current (2.1) at a dust grain.

3. Numerical results

First we compare the EEDF for a dusty plasma with that for a pristine plasma. In Fig. 1(a) the EEDFs of the two cases are presented for $R = L = 10$ cm, $a_d = 200$ nm, $n_d = 10^8$ cm^{-3}, $p_0 = 100$ mTorr, and $P_{in} = 500$ W. The discharge conditions were chosen to generate a Druyvesteyn-like EEDF in the pristine plasma according to earlier experimental evidence and modeling results [10, 11, 18]. One sees that in the dusty plasma the number of high-energy ($u \geq 15$ eV) electrons in the EEDF is higher than that in the pristine case. This can be attributed to the collection

https://doi.org/10.1017/S002237780400354X Published online by Cambridge University Press

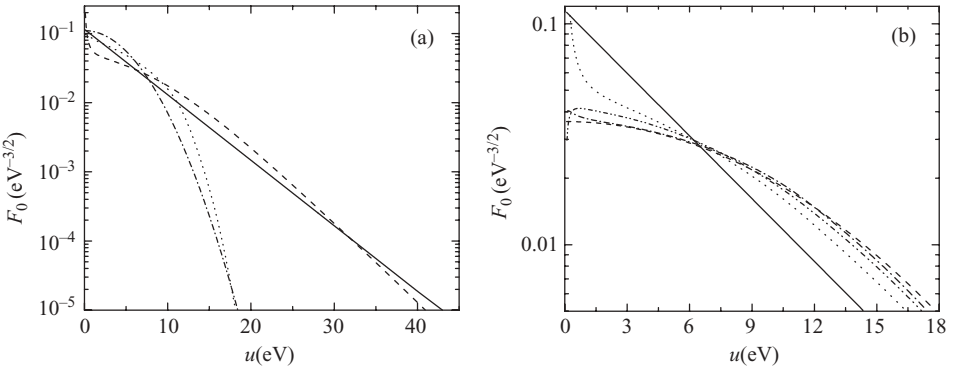


Figure 1. (a) The EEDFs for pristine (dotted curve) and dusty (dashed curve) argon plasma at $p_0 = 100$ mTorr, with $P_{in} = 500$ W, $R = L = 10$ cm, $a_d = 200$ nm and $n_d = 10^8$ cm^{-3}. The Druyvesteyn EEDF (dash-dotted curve) for pristine and Maxwellian EEDF (solid line) for dusty plasmas are also given. (b) The EEDFs calculated neglecting elastic and inelastic electron–dust collisions (dash-dotted curve), including only elastic electron–dust collisions (dash-dot-dotted curve), and including elastic and inelastic electron–dust collisions (dotted curve). The Druyvesteyn (dashed curve) and Maxwellian (solid curve) EEDFs are also shown.

of the plasma electrons by the dust grains, leading to a higher total electron loss in the complex plasma glow. To compensate this loss, the ionization intensifies by the elevated E_p giving rise to higher proportions of high-energy electrons in the EEDF tail. We have $E_p = 200.8$ and 2066.7 V m^{-1} for the pristine and dusty plasmas, respectively. The difference in the EEDFs also leads to a relatively high T_{eff} in the grain-loaded discharge. In fact, $T_{eff} = 3.74$ and 5.56 eV for $n_d = 0$ and 10^8 cm^{-3}, respectively. Figure 1(a) also shows that in the dust-free plasma, the EEDF is close to the Druyvesteyn distribution, but in the plasma with relatively high n_d ($\sim 10^8$ cm^{-3}) it becomes almost Maxwellian.

The Maxwellization of the EEDF at high dust densities can be attributed to electron–dust collisions. To see the effect of electron–dust collisions on the EEDF we compare the calculated EEDF for $\nu_{ed}^e \neq 0$ and $\nu_{ed}^c = 0$ with that obtained for $\nu_{ed}^e = 0$ and $\nu_{ed}^c = 0$. The EEDFs are shown in Fig. 1(b). We see that the EEDF for $\nu_{ed}^e \neq 0$ and $\nu_{ed}^c = 0$ practically coincides with that for $\nu_{ed}^e = 0$, $\nu_{ed}^c = 0$. This is because here the contribution of elastic collisions (proportional to m_e/m_d) in $S_{ed}(F_0)$ is small here.

For $\nu_{ed}^e \neq 0$ and $\nu_{ed}^c \neq 0$, the number of electrons with $-\phi_s \leq u \leq 33$ eV decreases compared with the $\nu_{ed}^c = 0$ cases, since electrons are now collected by the dust grains. The decrease of mid-energy electrons is accompanied by an increase of low- and high-energy ($u \geq 33$ eV) electrons (Fig. 1(b)). That is, inelastic electron–dust collisions move the electron EEDF towards Maxwellian.

The EEDF as well as the other plasma parameters depend strongly on n_d and a_d. We have calculated the EEDFs for given n_d for $a_d = 50$, 250, 500 and 750 nm. Some of the results are shown in Table 1. The corresponding Maxwellian and Druyvesteyn EEDFs are also calculated by setting $F_0(u) = c_1 \exp(-c_2 u^x)$, where c_1 and c_2 are constants and $x = 1, 2$ for the Maxwellian and Druyvesteyn EEDFs, respectively. It is found that for the conditions considered, the EEDF is close to Druyvesteyn for small (50–250 nm) a_d.

As a_d increases, because of electron–dust collisions the number of electrons in the mid-energy range ($-\phi_s \leq u \leq 20$ eV) decreases as compared with that of

https://doi.org/10.1017/S002237780400354X Published online by Cambridge University Press

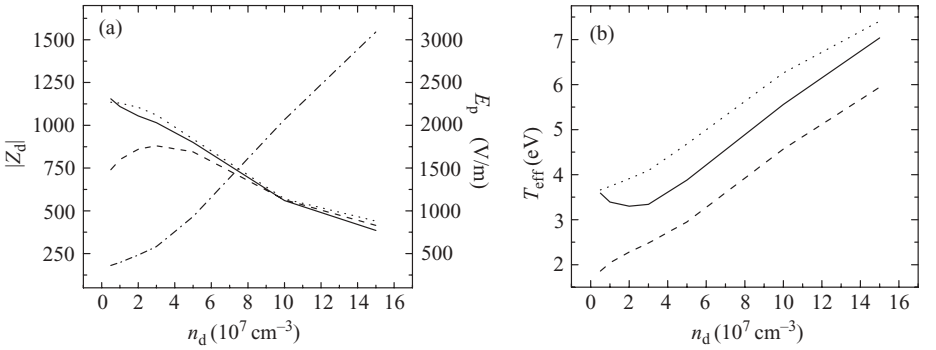


Figure 2. (a) The dust charge $|Z_d|$ versus the dust density n_d calculated from (2.2) (solid curve) and from the Maxwellian (dashed curve) and Druyvesteyn (dotted curve) EEDFs. The electric field E_p (dash-dotted curve) sustaining the plasma is also shown. (b) The effective electron temperature T_{eff} (solid line) for the EEDF calculated using (2.2) and the Druyvesteyn (dotted curve) and Maxwellian (dashed curve) EEDFs. The discharge conditions are the same as in Fig. 1.

the Druyvesteyn distribution, and at sufficiently high a_d (and/or n_d), the EEDF becomes close to Maxwellian. An increase in a_d is accompanied by an increase in the number of electrons in the tail of the EEDF. This change of the EEDF in the high-energy regime ($u \geq 20$ eV) with a_d can be attributed to inelastic electron–dust collisions. Indeed, with an increase of a_d the total electron loss (to the dust grains as well as the plasma wall) grows, the system then self-organizes to maintain a balance between production and loss of electrons by increasing the number of electrons in the tail of the EEDF. The increase of electrons in the tail is due to an increase of the electric field E_p, which sustains the plasma. In fact, the dust density has a similar effect on the EEDF. It can be shown that the EEDF also changes from Druyvesteyn to Maxwellian as n_d increases [5]. The variations of $|Z_d|$ and E_p with respect to n_d are shown in Fig. 2(a). In Table 1, the results from our model are listed together with that from the Maxwellian and Druyvesteyn distributions for selected dust sizes.

As can be seen from Fig. 2(b) and Table 1, the change in the EEDF with n_d and a_d can significantly affect the T_{eff} and the other plasma parameters, especially Z_d and n_e and n_i. We also note that at relatively low n_d (or a_d), Maxwellization of the EEDF due to an increase of n_d and/or a_d is accompanied by a decrease of T_{eff}. However, at relatively high n_d and/or a_d, the T_{eff} grows with the latter.

With an increase of a_d or n_d, the total dust surface collecting electrons and ions is enhanced. Therefore, the dust charge density $n_d|Z_d|$ also increases, as shown in Table 1. Due to the enhanced loss to the dust grains, at relatively high n_d (or a_d) n_e decreases dramatically with n_d (a_d). At low dust density ($n_d \leq 10^7$ cm^{-3}) or small dust radius ($a_d \leq 250$ nm), the change of n_e with n_d (a_d) is small. The ion density n_i depends on n_d (a_d) significantly weaker than n_e and $n_d|Z_d|$. For n_d in the range 0.5–15 $\times 10^7$ cm^{-3}, the range of n_i is only 5.95–7.3 $\times 10^{10}$ cm^{-3}.

From Table 1 and Fig. 2(a), one can also see that for relatively low dust densities ($n_d < 9 \times 10^7$ cm^{-3}) or small dust size ($a_d \leq 500$ nm), n_e, n_i and $n_d e|Z_d|$ are closer to the values obtained from the corresponding Druyvesteyn distribution than those from the corresponding Maxwellian distribution. On the other hand, at higher dust

https://doi.org/10.1017/S002237780400354X Published online by Cambridge University Press

densities ($n_d \geq 10^8$ cm^{-3}) or dust size ($a_d \sim 750$ nm) the parameters obtained from the calculated EEDF are close to that from the corresponding Maxwellian.

4. Discussion

Our numerical results show that the presence of dusts can strongly affect the EEDF in a plasma. They can cause major changes in the EEDF. In particular, an originally Druyvesteyn-like EEDF can become Maxwellian if the total dust charge is high. The fact that non-Maxwellian electrons can be thermalized by adding dusts is unexpected, since dusty plasmas are usually associated with disruption of thermalization because of: (a) inelastic electron–dust collisions, which often result in electron capture by the dusts; (b) substantial depletion of n_e, thus decreasing the electron–electron collision rate; and (c) higher T_{eff}, thus increasing the inelastic electron–neutral collision rate.

A clue to what to expect from the dust-modified EEDF is in the apparent reshaping and 'damping' [23] of the EEDF because of an increase of the high-energy tail and an overall depletion of the electron population. In general, there is competition between the main and the high-energy tail of the EEDF in the modification of T_{eff}. When the average energy of the main electrons increases or does not change, an increase of T_{eff} can be expected. However, when the average energy of the main electrons decreases (which can happen because of EEDF damping [23]), one expects a fall in T_{eff}. The latter apparently occurred in our example in Sec. 3. However, this behavior may be density-profile dependent, and should be investigated in more detail.

In the pristine plasma, Maxwellization of the EEDF is mainly due to electron–electron collisions [10]. Our results (Fig. 1) show that the inelastic electron–dust collisions reduce the number of electrons with $-\phi_s \leq u \leq 33$ eV, and this contributes to the enhanced electron thermalization, as can be seen in Fig. 1(b). However, it is not clear whether dusts can also de-thermalize a plasma.

As mentioned, the evolution of the EEDF can depend on the model. For example, with fixed E_p/N, one finds that T_{eff} inevitably decreases when the total grain charge increases [17, 23]. On the other hand, if the EEDF is fixed to either Maxwellian or Druyvesteyn, one always obtains an increase in T_{eff} (Table 1). Finally, if E_p/N is computed self-consistently as in our model, it appears that T_{eff} decreases at small $n_d a_d$, but increases if the latter is sufficiently large. Similarly, the density profiles can also strongly affect the behavior of T_{eff}.

Table 1 suggests that fixing the EEDF profile results in a rise of T_{eff} even for low dust density. This can be attributed to the fact that self-consistent redistribution of the low- and high-energy electrons is excluded in any model that employs a fixed EEDF profile. So that the only option for sustaining the necessary ionization is to increase T_{eff}. That is, by pre-selecting (usually estimated from the relation $E_p \sim (P_{in}/\sigma_p)^{1/2}$) the EEDF profile one effectively ignores the effect of E_p on the re-distribution of the electrons.

It should be pointed out that the present model still lacks several physical features that can be important in certain problems. For example, the OML theory will have to be improved in order to take care of very small dust grains. Future work should take into account a more realistic inhomogeneous spatial distribution of the dust charge and the plasma densities corresponding to the real discharges. For this, the reactive particulate-generating chemistries of the plasma components

https://doi.org/10.1017/S002237780400354X Published online by Cambridge University Press

Table 1. Effect of dust size variation on the plasma parameters for the self-consistent (calculated using (2.2)), Maxwellian and Druyvesteyn EEDFs. Here $n_d = 10^7$ cm^{-3} and the other conditions are the same as that for Fig. 1(a).

a_d (nm)	Parameter	Self-consistent	Druyvesteyn	Maxwellian
0	n_i, n_e (10^{11} cm^{-3})	1.064	2.03	6.12
	T_{eff} (eV)	3.74	2.98	1.63
	E_p (V m^{-1})	200.8	—	—
250	n_i (10^{10} cm^{-3})	7.04	5.77	11.1
	n_e (10^{10} cm^{-3})	5.68	4.35	10.0
	$n_d\|Z_d\|$ (10^{10} cm^{-3})	1.36	1.42	1.1
	T_{eff} (eV)	3.32	3.83	2.36
	E_p (V m^{-1})	434	—	—
750	n_i (10^{10} cm^{-3})	3.08	3.04	3.15
	n_e (10^{10} cm^{-3})	0.27	0.21	0.35
	$n_d\|Z_d\|$ (10^{10} cm^{-3})	2.81	2.83	2.8
	T_{eff} (eV)	5.45	6.46	4.69
	E_p (V m^{-1})	2285	—	—

(e.g. CH_4, SiH_4, C_2H_2, C_xF_y and their mixtures with Ar, H_2, etc.) and the charge variations of the nanosize grains should be considered.

Acknowledgements

This work was supported by the Humboldt Foundation, the Australian Research Council, the University of Sydney, Agency for Science, Technology and Research (A*STAR), and the Lee Kuan Yew Foundation. We would also like to thank M. Kushner, J. Goree, L. Tsendin, L. Boufendi and L. Stenflo for stimulating comments and discussions.

References

[1] Thomas, H. M. and Morfill, G. E. 1996 *Nature* **379**, 806.

[2] Bouchoule, A. (ed.). 1999 *Dusty Plasmas: Physics, Chemistry and Technological Impacts in Plasma Processing*. New York: Wiley.

[3] Hollenstein, Ch. 2000 *Plasma Phys. Control. Fusion* **42**, R93.

[4] Vladimirov, S. V. and Ostrikov, K. 2004 *Phys. Rep.* **393**, 175.

[5] Denysenko, I., Yu, M. Y., Ostrikov, K., Azarenkov, N. A. and Stenflo, L. 2004 *Phys. Plasmas* **11**, 4959.

[6] Boufendi, L. and Bouchoule, A. 2002 *Plasma Sources Sci. Technol.* A **11**, 211.

[7] Li, Y. J. T. 1996 Etching. *ULSI Technology* (ed. C. Y. Chang and S. M. Sze). New York: McGraw-Hill, pp. 329–370.

[8] Oehrlein, G. S. 2003 *Plasma Processing of Electronic Materials*. Berlin: Springer.

[9] Lieberman, M. A. and Lichtenberg, A. J. 1994 *Principles of Plasma Discharges and Materials Processing*. New York: Wiley.

[10] Godyak, V. A., Piejak, R. B. and Alexandrovich, B. M. 1992 *Phys. Rev. Lett.* **68**, 40.
Godyak, V. A., Piejak, R. B. and Alexandrovich, B. M. 1995 *Plasma Sources Sci. Technol.* **4**, 332.

[11] Smolyakov, A. I., Godyak, V. and Tyshetskiy, Y. 2001 *Phys. Plasmas* **8**, 3857.

[12] Sugai, H., Ghanashev, I., Hosokawa, M., Misuno, K., Nakamura, K., Toyoda, H. and Yamauchi, K. 2001 *Plasma Sources Sci. Technol.* **10**, 378.

https://doi.org/10.1017/S002237780400354X Published online by Cambridge University Press

[13] Xu, S., Ostrikov, K. N., Li, Y., Tsakadze, E. and Jones, I. R. 2001 *Phys. Plasmas* **8**, 2549.

[14] Kolobov, V. I. and Godyak, V. A. 1995 *IEEE Trans. Plasma Sci.* **23**, 503.

[15] Kortshagen, U., Busch, C. and Tsendin, L. D. 1996 *Plasma Sources Sci. Technol.* **5**, 1.

[16] Fridman, A. A., Boufendi, L., Hbid, T., Potapkin, B. N. and Bouchoule, A. 1996 *J. Appl. Phys.* **79**, 1303.

[17] Wang, D. and Dong, J. Q. 1997 *J. Appl. Phys.* **81**, 38.

[18] Denysenko, I., Yu, M. Y., Ostrikov, K. and Smolyakov, A. 2004 *Phys. Rev.* E **70**, 046403.

[19] Bouchoule, A. and Boufendi, L. 1993 *Plasma Sources Sci. Technol.* **2**, 204.

[20] Shkarofsky, I. P., Johnston, T. W. and Bachynski, M. P. 1966 *The Particle Kinetics of Plasma*. Reading, MA: Addison-Wesley.

[21] Biberman, L. M., Vorobev, V. S. and Yakubov, I. T. 1982 *Kinetics of Nonequilibrium Low-Temperature Plasma*. Nauka: Moscow.

[22] Gudmundsson, J. T. 2001 *Plasma Sources Sci. Technol.* **10**, 76.

[23] McCaughey, M. J. and Kushner, M. J. 1991 *J. Appl. Phys.* **69**, 6952.

https://doi.org/10.1017/S002237780400354X Published online by Cambridge University Press